

High Selectivity Bandpass Filter Using Three Pairs of Coupled Lines Loaded with Shorted Stubs

Kai-Da Xu^{1,2,3,*} and Fengyu Zhang^{1,2}

¹Department of Electronic Science, Xiamen University, Xiamen, 361005, China

²Shenzhen Research Institute of Xiamen University, Shenzhen 518057, China

³Department of Electrical and Computer Engineering, University of Wisconsin–Madison, Madison, WI 53706, USA
kaidaxu@ieee.org

Abstract — A high selectivity bandpass filter with multiple transmission poles (TPs) and transmission zeros (TZs) has been presented. By employing three pairs of parallel-coupled lines and two shorted stubs, sharp roll-off skirts and high stopband rejections can be achieved with five TPs and ten TZs. Theoretical analysis is explained and simulated results are illustrated on this high-performance filter. Finally, a bandpass filter example with center frequency of 2.15 GHz and 3-dB fractional bandwidth of 19% is designed, fabricated, and measured. It is shown that the measured transition band roll-off rates are better than 425 dB/GHz. Good agreement between the simulations and measurements validates the design method.

Index Terms — Bandpass filter, parallel-coupled lines, roll-off rates, shorted-circuit stubs, transmission poles, transmission zeros.

I. INTRODUCTION

Microstrip bandpass filters (BPFs) have drawn much attention to researchers due to their simple structure, small size, and easy fabrication. In recent years, BPFs using parallel-coupled lines are widely studied because the high accuracy and consistency of the filter circuit can be easily guaranteed [1-3]. Various structures using parallel-coupled lines loaded with stubs are designed for constructing high-performance filters, including open/shorted stubs [4-6], stepped-impedance stubs [7-9], and open/shorted coupled lines [10, 11]. Although wideband characteristics has been achieved in many filter designs, high frequency selectivity and excellent stopband suppression are facing the challenge due to lack of transmission zeros (TZs). In order to realize more pairs of TZs in the stopband, dual-mode ring resonators loaded with open stubs and open/shorted coupled lines have been proposed in [12]. However, this design method leads to large size of the filter circuit, which cannot meet the requirements of miniaturization.

In this paper, a high-selectivity BPF using three pairs of coupled lines loaded with two shorted stubs is

proposed. Compared with our previous work [13], this BPF can generate two more TZs in the stopband by employing two quarter-wavelength shorted stubs to the $3\lambda_g/4$ parallel coupled lines. Therefore, sharper roll-off skirts and high out-of-band rejection can be achieved with five TPs and ten TZs. For demonstration, a filter example with 3-dB fractional bandwidth (Δf) of 19% and operating center frequency at 2.15 GHz is fabricated, whose simulated and measured results are in good agreement.

II. BPF STRUCTURE AND DESIGN

Figure 1 shows the ideal circuit of the proposed BPF with three pairs of parallel-coupled lines and two shorted stubs, which can achieve high performance of ten TZs and five TPs. A pair of $\lambda_g/4$ parallel-coupled lines (even/odd-mode characteristic impedance Z_{0e2} , Z_{0o2} , electrical length θ , $\theta=90^\circ$ at the center frequency of f_0) in the middle are cascaded with two pairs of $3\lambda_g/4$ parallel-coupled lines (even/odd-mode characteristic impedance Z_{0e1} , Z_{0o1} , electrical length 3θ) at two sides. Two shorted stubs (characteristic impedance Z_1 , electrical length θ) are loaded on the end of two pairs of $3\lambda_g/4$ parallel-coupled lines, respectively. The characteristic impedances of the two feed lines at the input/output ports are both Z_0 . For further demonstration, theoretical analysis and design of the high selectivity BPF will be illustrated below.

The comparisons of the simulated transmission and reflection coefficients between the proposed BPF (i.e., BPF loaded with shorted stubs) and the BPF in [13] (i.e., BPF without shorted stubs) are shown in Figs. 2 (a) and (b), respectively. There are five TPs located at the two sides of the operating frequency $f_0=1$ GHz for generating a passband. Besides, ten TZs within the stopband are achieved. The impedance matrix deduction can be used for analyzing this BPF circuit. From Fig. 1, we can obtain that $V_2 = V_5$, $I_2 = -I_5$, $V_3 = V_8$, $I_3 = -I_8$, $V_6 = V_9$, $I_6 = -I_9$, $V_7 = V_{12}$, $I_7 = -I_{12}$, and $I_4 = I_{11} = -jV_4/(Z_1 \tan \theta)$. $[Z]^a$ and $[Z]^b$ denote the impedance matrix of the $3\lambda_g/4$ and $\lambda_g/4$ parallel-coupled lines, respectively. The overall impedance matrix Z' of the filter can be calculated as:

$$\begin{bmatrix} V_1 \\ V_{10} \end{bmatrix} = \begin{bmatrix} Z'_{11} & Z'_{12} \\ Z'_{21} & Z'_{22} \end{bmatrix} \begin{bmatrix} I_1 \\ I_{10} \end{bmatrix}. \quad (1)$$

The reflection coefficient S_{11} and transmission coefficient S_{21} can be expressed as:

$$S_{11} = \frac{(Z'_{11} - Z_0)(Z'_{22} + Z_0) - Z'_{12}Z'_{21}}{(Z'_{11} + Z_0)(Z'_{22} + Z_0) - Z'_{12}Z'_{21}},$$

and

$$S_{21} = \frac{2Z'_{21}Z_0}{(Z'_{11} + Z_0)(Z'_{22} + Z_0) - Z'_{12}Z'_{21}}. \quad (2)$$

Based on the impedance matrix deduction, TPs can be calculated by setting $S_{11}=0$. Through calculation, five TPs can be obtained and illustrated as below:

$$f_{p1} = \frac{2f_0}{\pi} \cos^{-1} \sqrt{\frac{Z_{0e1} - 2Z_{0o2} + Z_{0o1}}{2Z_{0e1} + 4Z_{0o2} + 2Z_{0o1}}}, \quad (3)$$

$$f_{p2} = \frac{2f_0}{\pi} \cos^{-1} \sqrt{\frac{Z_{0e1} - 2Z_{0e2} + Z_{0o1}}{2Z_{0e1} + 4Z_{0e2} + 2Z_{0o1}}}, \quad (4)$$

$$f_{p3} = f_0, \quad (5)$$

$$f_{p4} = \frac{2f_0}{\pi} (\pi - \cos^{-1} \sqrt{\frac{Z_{0e1} - 2Z_{0e2} + Z_{0o1}}{2Z_{0e1} + 4Z_{0e2} + 2Z_{0o1}}}), \quad (6)$$

$$f_{p5} = \frac{2f_0}{\pi} (\pi - \cos^{-1} \sqrt{\frac{Z_{0e1} - 2Z_{0o2} + Z_{0o1}}{2Z_{0e1} + 4Z_{0o2} + 2Z_{0o1}}}). \quad (7)$$

Compared with our previous work, i.e., BPF without shorted stubs, this proposed BPF can generate ten TZs, the four TZs f_{tz1} , f_{tz4} , f_{tz7} and f_{tz10} keep unchanged whose positions can be expressed as

$$f_{tz1} = 0, \quad f_{tz4} = \frac{2}{3}f_0, \quad f_{tz7} = \frac{4}{3}f_0, \quad f_{tz10} = 2f_0. \quad (8)$$

Another six TZs within the stopband at the frequency range from 0 to $2f_0$ can be obtained through calculation by setting transmission coefficient $S_{21}=0$. Moreover, the positions of the two TZs f_{tz5} and f_{tz6} are located more close to the passband than the BPF without shorted stubs, as seen in Fig. 2 (a). Thus, the roll-off skirts of the passband will become sharper to further improve frequency selectivity.

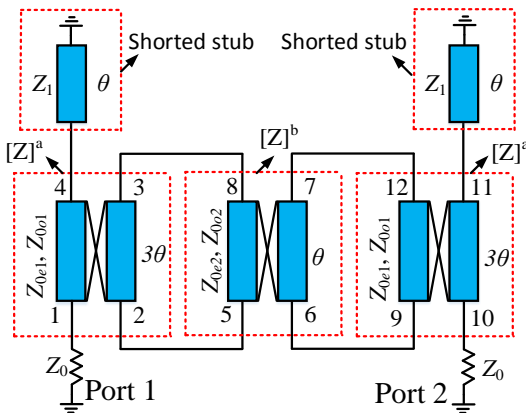


Fig. 1. Ideal circuit of the BPF with ten TZs.

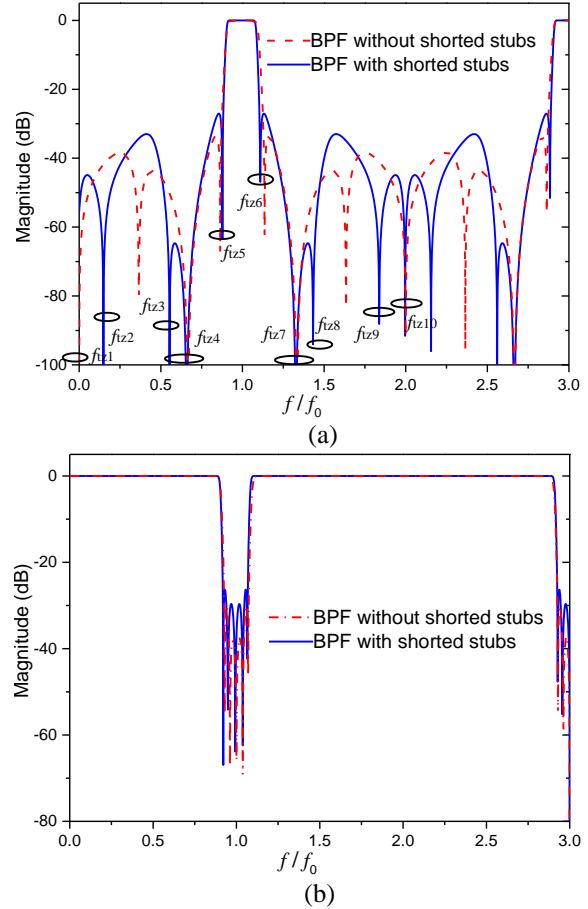


Fig. 2. Simulated results on ideal circuit of (a) S_{21} and (b) S_{11} with $\theta=90^\circ$, $Z_0=50 \Omega$, $Z_1=160 \Omega$, $Z_{0e1}=158 \Omega$, $Z_{0o1}=60 \Omega$, $Z_{0e2}=109 \Omega$, $Z_{0o2}=66 \Omega$.

Figure 3 illustrates the simulated $|S_{21}|$ against Z_1 and k_2 [$k_2 = (Z_{0e2} - Z_{0o2}) / (Z_{0e2} + Z_{0o2})$]. Seen from Figs. 3 (a) and (b), the four TZs f_{tz1} , f_{tz4} , f_{tz7} and f_{tz10} remain unchanged as the parameters Z_1 and k_2 shift, whereas the other six TZs f_{tz2} , f_{tz3} , f_{tz5} , f_{tz6} and f_{tz8} , and f_{tz9} will be adjusted. The 3-dB fractional bandwidth Δf almost keep unchanged as Z_1 varies, In contrast, when k_2 varies slightly, Δf will be changed very obviously.

Except for the TPs, TZs and Δf , the concerned characteristics of BPF mainly include maximal out-of-band $|S_{21}|$ (T_s), maximal in-band $|S_{11}|$ (T_p) [4] and transition band roll-off rate (ξ_{ROR}) [5]. Figures 4 (a), (b), (c) show the corresponding variations of Δf , T_s and T_p against the parameters Z_1 , k_1 and k_2 , respectively, where $k_1 = (Z_{0e1} - Z_{0o1}) / (Z_{0e1} + Z_{0o1})$, $k_2 = (Z_{0e2} - Z_{0o2}) / (Z_{0e2} + Z_{0o2})$. As seen in Fig. 4 (a), T_s and T_p will both decrease when Z_1 increases, which indicates that both of the in-band and out-of-band characteristics will be improved. When the parameter k_1 increases as seen in Fig. 4 (b), T_s will grow up slightly but T_p will decrease and then rise up, while the bandwidth Δf will fall down from 18.6% to 17.4% directly. In contrast, as k_2 increases, T_s will almost

remain unchanged but T_p will reduce and then go up, while Δf will rise up simultaneously as seen in Fig. 4 (c). Note that the Δf will be rise from 16% to 20% when k_2 increases under the return loss condition of over 10 dB within the passband. Consequently, it indicates that the 3-dB fractional bandwidth of the filter is mainly determined by the pair of $\lambda g/4$ coupled lines. In addition, due to the minimum dimension limitation of the fabrication, the width of the microstrip line and the gap of coupled lines must be no smaller than 0.1 mm on the substrate.

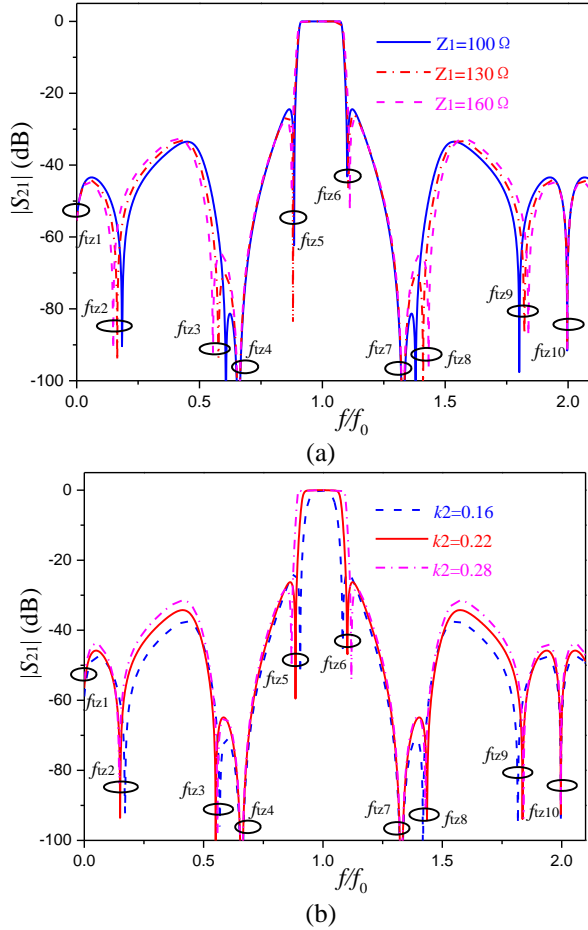


Fig. 3. Simulated $|S_{21}|$ (a) versus Z_1 , where $Z_{0e1}=158 \Omega$, $Z_{0o1}=60 \Omega$, $Z_{0e2}=109 \Omega$, $Z_{0o2}=66 \Omega$; and (b) versus k_2 , where $Z_1=160 \Omega$, $Z_{0e1}=158 \Omega$, $Z_{0o1}=60 \Omega$, $Z_{0e2}=109 \Omega$.

From the above analysis, it is observed that the parameter k_2 affects the Δf and T_p . On the other hand, it is also related to the coupling coefficient between the two one-wavelength ring resonators, thereby having impact on the in-band characteristics. The coupling coefficient can be expressed as [14]:

$$k = \frac{f_{ip5}^2 - f_{ip1}^2}{f_{ip5}^2 + f_{ip1}^2}. \quad (9)$$

where f_{ip1} and f_{ip5} denote the first and last transmission poles, respectively. Taking the layout in Fig. 5 (a) for instance, as shown in Fig. 5 (b), the coupling coefficient will increase slightly to the peak and then decrease when s_1 increases. Moreover, Fig. 5 (c) illustrates the external quality factor Q_e variation with the change of s_2 , where Q_e will increase gradually and become flat as s_2 increases.

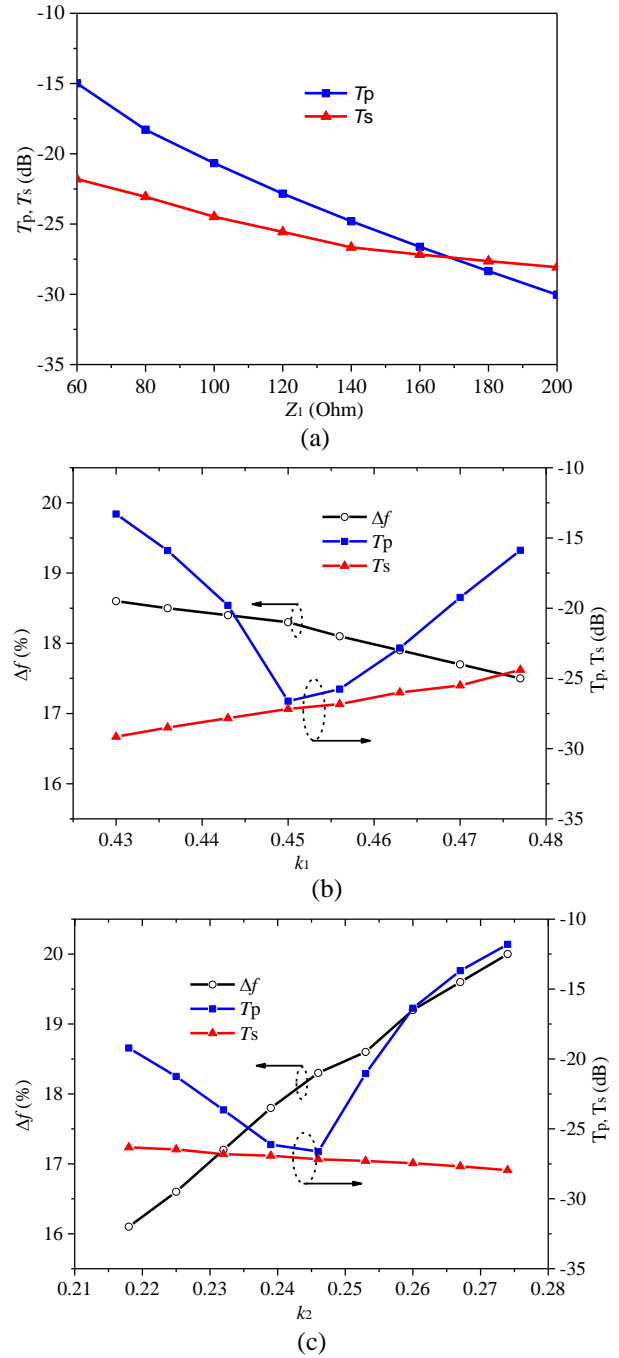


Fig. 4. Calculated Δf , T_s and T_p , (a) versus Z_1 , (b) versus k_1 , and (c) versus k_2 .

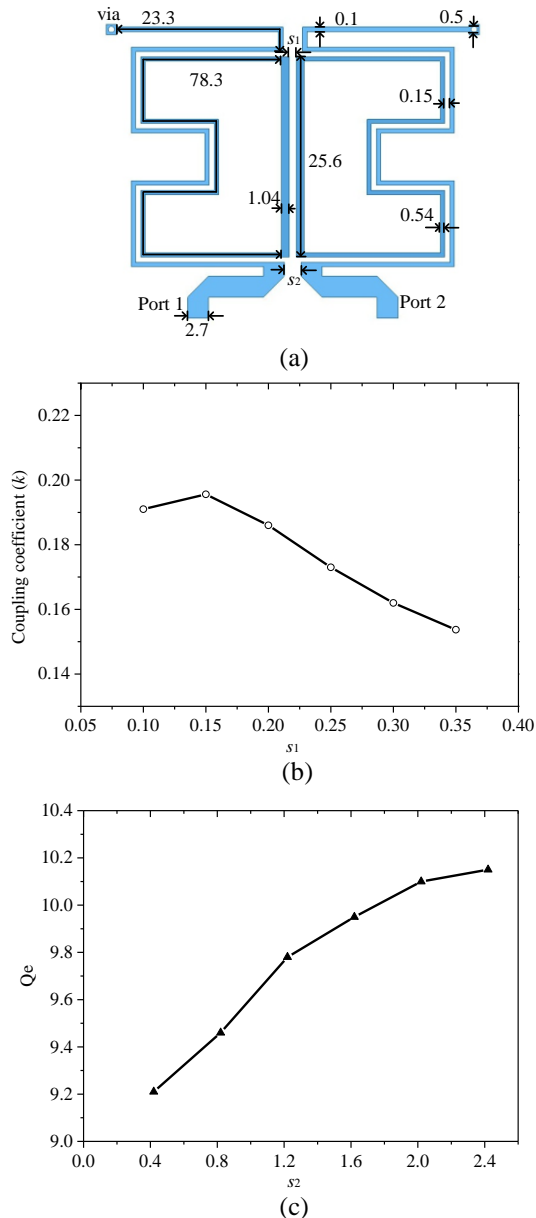


Fig. 5. (a) Layout of the proposed BPF (unit: mm, substrate: relative permittivity of 2.65, thickness of 1 mm), (b) coupling coefficient k changes with the value of s_1 , where $s_2=1.62$ mm, and (c) external quality factor Q_e changes with the value of s_2 , where $s_1=0.42$ mm.

III. EXPERIMENTAL RESULTS

According to the analysis and discussion above, a bandpass filter with center frequency at 2.15 GHz is designed. The final parameters for the filter circuit in Fig. 1 are: $Z_0=50 \Omega$, $Z_{0e1}=158 \Omega$, $Z_{0o1}=60 \Omega$, $Z_{0e2}=109 \Omega$, $Z_{0o2}=66 \Omega$, $Z_1=160 \Omega$ and $\theta=90^\circ$. Furthermore, the 3-dB bandwidth is chosen as 19%, and the printed bandpass filter prototype is fabricated on the substrate with relative permittivity of 2.65 and thickness of 1 mm as illustrated

in Fig. 5 (a), where $s_1=0.42$ mm and $s_2=1.62$ mm. Figure 6 shows the photograph of the fabricated filter.

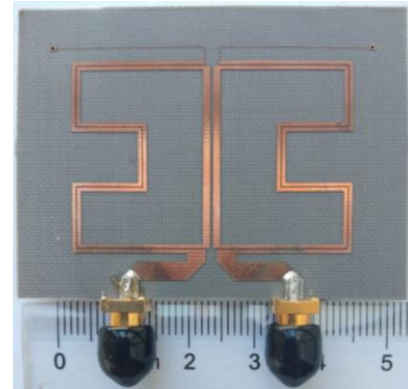


Fig. 6. Photograph of the fabricated BPF.

The simulated and measured results of Fig. 6 are shown in Fig. 7, which are in good agreement. The measured insertion losses are less than 1.8 dB while the return losses are greater than 11.5 dB within the passband (1.98–2.33 GHz). The simulated lower and upper transition band roll-off rates ζ_{ROR} are both better than 486 dB/GHz, while the measured counterparts are both over 425 dB/GHz. In addition, over 31 dB lower stopband can be achieved, while the upper stopband rejection is more than 23 dB from 2.41 to 4.24 GHz. Besides, due to the existing second harmonic around 4.49 GHz, the stopband rejection is over 13 dB from 2.41 to 6 GHz.

Table 1 tabulates the performance comparisons of the proposed BPF with some previous works, and it can be seen that the presented study has sharper roll-off skirts to realize high frequency selectivity with ten TZs. Compared with some previous BPFs, not only more TZs can be realized for improving stopband rejection, but also high transition band roll-off rates can be obtained in this BPF.

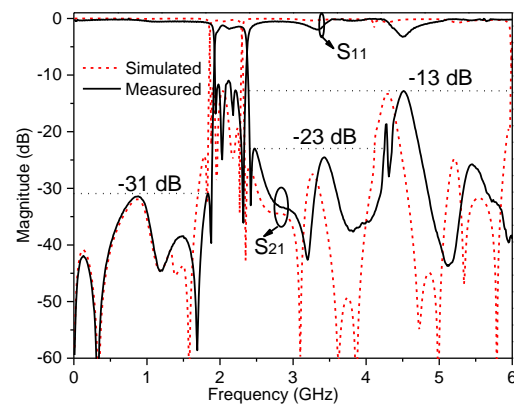


Fig. 7. Simulated and measured S-parameters of the BPF.

Table 1: Performance comparisons with some previous BPFs

	TPs	TZs	Δf	ξ_{ROR}^* (L/U) (dB/GHz)	Upper Stopband (dB)	Circuit Size $\lambda_g \times \lambda_g^{**}$
[4]-I	5	6	61.7%	175/213	>15 (2.7 f_0)	0.68×0.53
[5]	7	4	78%	288/175	>35.1 (2.6 f_0)	0.56×0.23
[7]-A	5	6	70%	81/121	>21 (2.6 f_0)	0.53×0.41
[7]-B	5	6	37%	94/120	>23 (2.8 f_0)	0.61×0.55
[12]	5	8	20.6%	175/340	>20 (2.9 f_0)	1.06×0.61
[13]	5	8	19%	340/425	>18 (3 f_0)	0.39×0.28
[15]	2	7	8.3%	130/215	>12 (2.6 f_0)	0.4×0.26
This work	5	10	19%	425/567	>23 (2.1f_0) >13 (3f_0)	0.49×0.28

Transition band roll-off rates $\xi_{\text{ROR}}^ = |\delta_{20\text{dB}} - \delta_{3\text{dB}}| / |f_{20\text{dB}} - f_{3\text{dB}}|$, where $\delta_{20\text{dB}}$ denotes the 20/3dB attenuation point, and $f_{20\text{dB}}$ is the 20/3dB passband frequency of $|S_{21}|$. L and U denote lower and upper transition band roll-off rates, respectively. ** λ_g : guided wavelength of the 50 Ω microstrip line at the center frequency.

IV. CONCLUSION

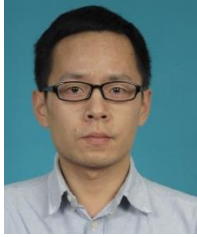
A high selectivity bandpass filter using three pairs of coupled lines loaded with shorted stubs has been presented in this paper. By employing three pairs of parallel-coupled lines and two shorted stubs, sharper roll-off skirts and good stopband rejections can be achieved with five TPs and ten TZs. Finally, the simulations and measurements of the demonstrative filter are in good agreement. The measured transition band roll-off rates can be up to 425 dB/GHz, which is much higher than those of the previous reported works.

ACKNOWLEDGMENT

This work was supported in part by the National Natural Science Foundation of China under Grant 61601390 and the Guangdong Natural Science Foundation under Grant 2016A030310375.

REFERENCES

- [1] T. Lopetegi, M. A. G. Laso, J. Hernandez, M. Bacaicoa, D. Benito, M. J. Garde, M. Sorolla, and M. Guglielmi, "New microstrip 'wiggly-line' filters with spurious passband suppression," *IEEE Trans. Microw. Theory Tech.*, vol. 49, pp. 1593-1598, 2001.
- [2] F. Karshenas, A. R. Mallahzadeh, and J. Rashed-Mohassel, "Size reduction and harmonic suppression of parallel coupled-line bandpass filters using defected ground structure," *ACES Journal*, vol. 25, pp. 149-155, 2010.
- [3] K. D. Xu, Y. Zhang, J. L. Li, W. T. Joines, and Q. H. Liu, "Miniaturized notch-band UWB bandpass filters using interdigital-coupled feed-line structure," *Microw. Opt. Technol. Lett.*, vol. 56, no. 10, pp. 2215-2217, Oct. 2014.
- [4] W. J. Feng, W. Q. Che, Y. M. Chang, S. Y. Shi, and Q. Xue, "High selectivity fifth-order wideband bandpass filters with multiple transmission zeros based on transversal signal-interaction concepts," *IEEE Trans. Microw. Theory Tech.*, vol. 61, no. 1, pp. 89-97, 2013.
- [5] K. D. Xu, F. Y. Zhang, Y. H. Liu, and W. Nie, "High selectivity seventh-order wideband bandpass filter using coupled lines and open/shorted stubs," *Electron. Lett.*, vol. 54, no. 4, pp. 223-225, 2018.
- [6] Y. J. Guo, X. H. Tang, and K. D. Xu, "Dual high-selectivity band-notched ultra-wideband filter with improved out-of-band rejection," *ACES Journal*, vol. 31, no. 9, pp. 1072-1078, 2016.
- [7] B. Zhang, Y. L. Wu, and Y. A. Liu, "Wideband single-ended and differential bandpass filters based on terminated coupled line structures," *IEEE Trans. Microw. Theory Tech.*, vol. 65, pp. 761-774, 2017.
- [8] Y. L. Wu, L. W. Cui, W. W. Zhang, L. X. Jiao, Z. Zhuang, and Y. Liu, "High performance single-ended wideband and balanced bandpass filters loaded with stepped-impedance stubs," *IEEE Access*, vol. 5, pp. 5972-5981, 2017.
- [9] X. Deng, K. D. Xu, Z. Wang, and B. Yan, "Novel microstrip ultra-wideband bandpass filter using radial-stub-loaded structure," *ACES Journal*, vol. 32, no. 12, pp. 1148-1151, 2017.
- [10] W. J. Feng, W. Q. Che, M. L. Hong, and Q. Xue, "Dual-band microstrip bandstop filter with multiple transmission poles using coupled lines," *IEEE Microw. Wireless Compon. Lett.*, vol. 27, no. 3, pp. 236-238, 2017.
- [11] K. D. Xu, D. Li, and Y. Liu, "High-selectivity wideband bandpass filter using simple coupled lines with multiple transmission poles and zeros," *IEEE Microw. Wireless Compon. Lett.*, vol. 29, no. 2, 2019. DOI: 10.1109/LMWC.2019.2891203
- [12] W. J. Feng, X. Gao, W. Q. Che, and Q. Xue, "Bandpass filter loaded with open stubs using dual-mode ring resonator," *IEEE Microw. Wireless Compon. Lett.*, vol. 25, pp. 295-297, 2015.
- [13] K. D. Xu, F. Zhang, Y. Liu, and Q. H. Liu, "Bandpass filter using three pairs of coupled lines with multiple transmission zeros," *IEEE Microw. Wireless Compon. Lett.*, vol. 28, no. 7, pp. 576-578, 2018.
- [14] J. S. Hong and M. J. Lancaster, *Microwave Filters for RF/Microwave Applications*. New York, NY, USA: Wiley, 2011.
- [15] K. Xu, Y. Zhang, Y. Fan, W. T. Joines, and Q. Liu, "Novel circular dual-mode filter with both capacitive and inductive source-load coupling for multiple transmission zeros," *J. Electromag. Waves Appl.*, vol. 26, pp. 1675-1684, 2012.



Kai-Da Xu received the B.S. and Ph.D. degrees in Electromagnetic Field and Microwave Technology from University of Electronic Science and Technology of China (UESTC), Chengdu, China, in 2009 and 2015, respectively.

From 2012 to 2014, he was a Visiting Researcher with the Department of Electrical and Computer Engineering, Duke University, Durham, NC, USA, under the financial support from the China Scholarship Council. From 2016 to 2017, he was a Postdoctoral Fellow with the State Key Laboratory of Terahertz and Millimeter Waves, City University of Hong Kong, Hong Kong. In 2015, he joined the Department of Electronic Science, Xiamen University, Xiamen, China as an Assistant Professor. Since 2018, he has been an Honorary Fellow with the Department of Electrical and Computer Engineering, University of Wisconsin–Madison, WI, USA. He has authored and coauthored over 100 papers in peer-reviewed journals and conference proceedings. He received the UESTC Outstanding Graduate Awards in 2009 and 2015,

respectively. He was the recipient of National Graduate Student Scholarship in 2012, 2013, and 2014 from Ministry of Education, China. Since 2014, he has served as a Reviewer for more than 30 journals including IEEE Transactions on Microwave Theory and Techniques, IEEE Transactions on Antennas and Propagation, IEEE Microwave and Wireless Components Letters and IEEE Antennas and Wireless Propagation Letters. Since 2017, he has served as an Associate Editor for both of the *IEEE Access* and *Electronics Letters*. He is also an Editorial Board Member of the *AEÜ-International Journal of Electronics and Communications*. His research interests include RF/microwave, mm-wave/THz devices and antenna arrays.



Fengyu Zhang was born in Fujian, China. He received the B.Sc. degree in Fuzhou University, Fujian, China, in 2016, and currently he is working toward the M.S. degree in Xiamen University. His research interests include RF/microwave components and circuits.